Journal of Porous Media, 14 (6): 555–563 (2011)

THERMAL NON-EQUILIBRIUM MODELING OF COUPLED HEAT AND MASS TRANSFER IN BULK ADSORPTION SYSTEM OF POROUS MEDIA

Xuewei Zhang & Wei Liu[*]

School of Energy and Power Engineering, Huazhong University of Science and Technology, Wuhan 430074, Peoples Republic of China

[*]Address all correspondence to Wei Liu E-mail: w_liu@hust.edu.cn

Original Manuscript Submitted: 10/13/2007; Final Draft Received: 10/26/2009

According to the volume-averaging method, a two-dimensional thermal non-equilibrium mathematical model was developed to simulate the coupled heat and mass transfer in porous media with strong adsorption, in which local fluid and solid temperatures were dealt with separately. The temperature-dependent Langmuir isotherm was applied to describe the equilibrium characteristics of binary gas CO_2 adsorbed by zeolite 13X. The adsorption-generated heat was considered in the energy equation of the solid matrix. The coupling of two energy equations was made by considering the interfacial heat transfer term. The adsorption feature of a packed bed filled with porous adsorbent and the effects of bulk flow velocity, particle diameter, effective thermal conductivity of solids, and specific heat of adsorbent on product concentration were investigated numerically. The numerical simulation shows that the heat transfer characteristic has notable effects on the quantity of adsorption and the purity of the product. High adsorption efficiency can be achieved by improving the adsorbent physical properties and reducing the temperature span of the pressure swing adsorption process. Experimental data reported by other researchers validate the accuracy of the present model.

KEY WORDS: *heat and mass transfer, non-equilibrium, porous media, pressure swing adsorption, carbon dioxide*

1. INTRODUCTION

Pressure swing adsorption (PSA) technology based on the adsorption characteristics of the components has been widely applied to separate gas mixtures. Recently, the PSA process with strong adsorption has attracted special attention in separating carbon dioxide, one of the most predominant greenhouse gases, from flue gas. This process is characterized by several unique features. First of all, mass transfer plays an important role in the periodic adsorption process under a rapid cycle condition. Second, the operating temperature span caused by absorption or release of adsorption-generated heat is commonly more than 10°C which leads to a significant change in adsorbed quantity. Finally, heat and mass transfer are coupled with each other. Therefore, it is necessary to consider both heat and mass transfer processes in analysis of the adsorber, especially in some large-scale PSA equipment (Steinbery, 1992; Kikkinides et al., 1993).

Heat and mass transfer in porous media have been investigated for several decades (Nield and Bejan, 1999). The local thermal equilibrium model (Cheng, 1978; Whitaker, 1986; Kim and Vafai, 1989; Rees and Vafai, 1999) and the local thermal non-equilibrium model (Quintard and Whitaker, 1993; Amiri and Vafai, 1998; Kim et al. 2000) have been used in dealing with heat transport in porous media. The former is relatively simple However it is valid only when the temperature difference between solid and fluid phases is very small The latter is relatively complex, as heat exchange between solid and fluid phases has to be considered. According to the criterion proposed by Kim and Jang (2002), the thermal non-

1091–028X/11/$35.00

NOMENCLATURE

B_i	Langmuir parameter (1/Pa)
Ra	Rayleigh number
Nu	Nusselt number
T	temperature (K)
t	time (s)
C_i	mass fraction of species i in the gas phase
C_f	specific heat of fluid [J/(kg/K)]
C_s	specific heat of solid [J/(kg/K)]
v	velocity (m/s)
u	uniform velocity
D_b	mass diffusivity (m^2/s)
d_p	particle diameter (m)
F	geometric function ($m^{-3/2}$)
H	adsorption heat (J/kg)
$h_{\rm sf}$	solid-to-fluid heat transfer coefficient [W/(m^2/K)]
$h_{m,\rm sf}$	solid-to-fluid mass transfer
h_v	volumetric solid-to-fluid
$h_{m,v}$	volumetric solid-to-fluid mass
K	permeability of porous media (m^2)
L	length of adsorber (m)
P	pressure (Pa)

Greek Symbols

φ	porosity of bed
ρ	density of fluid (kg/m^3)
ρ_b	density of bed (kg/m^3)
μ_f	viscosity of fluid [kg/(m/s)]
λ_f	thermal conductivity of coefficient [kg/(m^2/K)] fluid [W/(m/K)]
λ_s	thermal conductivity of heat transfer coefficient [W/(m^3/s)] solid [W/(m/K)]

Subscripts

eff	effective
i	species i
k	species number
$q_{\max,i}$	maximal adsorbed amount of species i (kg/kg)
q_i	adsorption quantity of species i (kg/kg)

Superscript

*	equilibrium state

equilibrium model should be used to describe the strong adsorption processes in the porous packed bed.

The simplest and most commonly applied mass transfer model is the linear driving force (LDF) model, which was first proposed by Glueckauf and Coates (1947). The LDF model was derived by assuming that the driving force of mass transfer within a chromatographic process takes on a simple linear form between the compositions in equilibrium with the bulk phase (Carta, 1993; Hsuen, 2000) Veldsink et al. (1995) adopted the Fick model and the dusty-gas model to the study mass transport process accompanied with the chemical reaction in a porous catalyst.

However, attention has not been fully paid to the effect of heat transfer on mass transfer for studying the coupling of heat and mass transfer in porous media subjected to chemical reactions or physical adsorption So, a mathematical model describing the coupled process of bulk adsorption has been established in this paper. Both the Forchheimer and Brinkman effects have been taken into account in the momentum equation The thermal non-equilibrium model has been adopted and two energy equations have been coupled with the interfacial heat transfer term, in which the adsorption-generated heat has been considered in the energy equation of the solid matrix. The temperature-dependent Langmuir isotherm has been used to describe the equilibrium characteristics of CO_2 and N_2, and the mass transfer coefficient has been approximated as the external mass transfer coefficient of the particle. The adsorption features of the packed bed also have been investigated numerically.

2. MATHEMATICAL MODELING

2.1 Problem Description

The schematic diagram of the physical model is shown in Fig. 1. The cylindrical bed with a 257 mm diameter and a length of 1000 mm was filled with a homogenous and isotropic spherical adsorbent subjected to a constant tem-

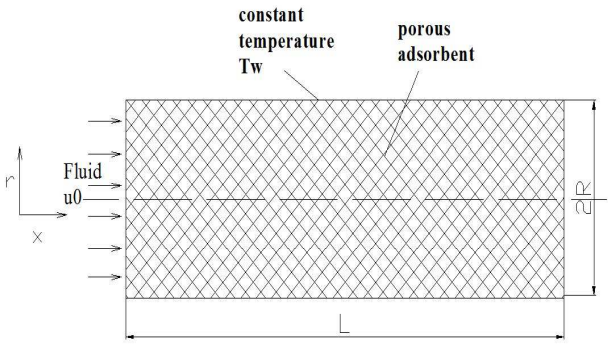

FIG. 1: Schematic diagram of a packed bed filled with zeolite 13X

perature boundary condition. The fluid was injected at a constant rate with uniform velocity u_0. Due to the symmetry of the packed bed, only half of it was considered in the numerical simulation

The following assumptions are made in the modeling:

1. Ideal gas law is applicable.
2. The temperature of a particle is uniform.
3. Natural convection and radiation heat transfer are neglected.
4. The physical properties of the gas phase, adsorbent and column wall are constant.
5. The heat capacity of the adsorbed gas is neglected.

Under the above assumptions, the governing equations are obtained as follows:

1. For overall mass balance:

$$\frac{\partial \varphi \rho}{\partial t} + \frac{\partial \rho u}{\partial x} + \frac{1}{\mathrm{r}} \frac{\partial (r \rho v)}{\partial r} + \rho_b \sum_{k=1}^{n} \frac{\partial q_k}{\partial t} = 0 \quad (1)$$

2. For mass balance for gas i (CO_2 or N_2):

$$\frac{\partial \varphi \rho C_i}{\partial t} + \frac{\partial}{\partial x}(\rho u C_i) + \frac{1}{r}\frac{\partial}{\partial r}(r \rho v C_i) - \frac{\partial}{\partial x} \times \left(D_b \frac{\partial C_i}{\partial x}\right) - \frac{1}{r}\frac{\partial}{\partial r}\left(r D_b \frac{\partial C_i}{\partial r}\right) + \rho_b \frac{\partial q_i}{\partial t} = 0 \quad (2)$$

3. For the Darcy–Forchheimer–Brinkman momentum equation (Sozen and Kuzay, 1996):

$$\rho_f \left(\frac{\partial \vec{V}}{\partial t} + \vec{V} \cdot \nabla \vec{V}\right) = -\nabla p + \mu_{\text{eff}} \nabla^2 \vec{V} - \frac{\mu_f}{K} \vec{V} - \rho_f \frac{F \varphi}{\sqrt{K}} \left|\vec{V}\right| \vec{V} \quad (3)$$

The second, third and fourth terms on the righthand side of Eq. (3) represent the viscous effect, frictional resistance and inertial force respectively.

ThepPermeability of the porous bed (Ergun, 1952) and geometric factor F in the momentum equation are given as (Quintard and Whitaker, 1993)

$$K = \frac{\varphi^3 d_p^2}{150 (1-\varphi)^2} \quad (4)$$

$$F = \frac{1.75}{150 \varphi^{3/2}} \quad (5)$$

The energy conservation equations for the fluid and solid matrix are given as

$$\frac{\partial [\varphi C_f \rho T_f]}{\partial t} + \frac{\partial (C_f \rho u T_f)}{\partial x} + \frac{1}{r}\frac{\partial (r C_f \rho v T_f)}{\partial r} = \frac{\partial}{\partial x}\left(\lambda_{f,\text{eff}} \frac{\partial T_f}{\partial x}\right) + \frac{1}{r}\frac{\partial}{\partial r}\left(r \lambda_{f,\text{eff}} \frac{\partial T_f}{\partial r}\right) + h_v (T_s - T_f) \quad (6)$$

$$\frac{\partial [C_s \rho_b T_s]}{\partial t} = \frac{\partial}{\partial x}\left(\lambda_{s,\text{eff}} \frac{\partial T_s}{\partial x}\right) + \frac{1}{r}\frac{\partial}{\partial r}\left(r \lambda_{s,\text{eff}} \frac{\partial T_s}{\partial r}\right) - h_v (T_s - T_f) + \sum_{k=1}^{n} H_k \rho_b \frac{\partial q_k}{\partial t} \quad (7)$$

The mass transfer is described by the LDF model,

$$\rho_b \frac{\partial q_i}{\partial t} = h_{m,v} (C_i - C_i^*) \quad (8)$$

The fluid and solid effective thermal conductivities are

$$\lambda_{f,\text{eff}} = \varphi \lambda_f \quad (9)$$

$$\lambda_{s,\text{eff}} = (1-\varphi) \lambda_s \quad (10)$$

The volumetric solid-to-fluid heat and mass transfer coefficients h_v and $h_{m,v}$ are

$$h_v = 6 h_{\text{sf}} (1-\varphi)/d_p \quad (11)$$

$$h_{m,v} = 6 h_{m,\text{sf}} (1-\varphi)/d_p \quad (12)$$

where heat transfer coefficient $h_{\rm sf}$ is given by (Wakao et al., 1979)

$$\begin{aligned} \mathrm{Nu} &= \frac{h_{\rm sf} d_p}{\lambda_f} = 2.0 + 1.1 \mathrm{Pr}^{1/3} \mathrm{Re}_p^{0.6} \\ \mathrm{Pr} &= \frac{C_p \mu}{k}, \quad \mathrm{Re}_p = \frac{\rho u d_p}{\mu} \end{aligned} \tag{13}$$

where Reynolds number Re_p covers the range up to 8500.

Mass transfer coefficient $h_{m,\rm sf}$ is given by

$$\begin{aligned} Sh &= \frac{D_i h_{m,\rm sf}}{D_m} = 2.0 + 0.6 Sc^{1/3} \mathrm{Re}^{1/2} \\ Sc &= \frac{\mu}{\rho_f D_m}, \quad \mathrm{Re} = \frac{\rho_f V \varphi d_f}{\mu} \end{aligned} \tag{14}$$

The temperature-dependent Langmuir isotherm (Harlick and Tezel, 2001) is used to represent the gas–solid equilibrium isotherm:

$$q_i = \frac{q_{\max,i} b_i p C_i^*}{1 + \sum_{k=1}^{n} b_k p C_k^*} \tag{15}$$

where $q_{\max,i} = B_{1,i} \exp(B_{2,i} T)$ and $b_i = B_{3,i} \exp(B_{4,i} T)$.

The parameter values used in the simulation are listed in Table 1, in which the Langmuir parameters for CO_2 and N_2 were measured by the constant volume method at different pressures (Suzuki, 1990).

The initial and boundary conditions are given as follows:

1. Initial conditions ($t = 0$):

$$\begin{aligned} &U = U_0, V = 0 \\ &T_f = T_s = T_w = 330\mathrm{K} \\ &C_{\mathrm{CO_2}} = 0, \quad C_{\mathrm{N_2}} = 1.0 \\ &q_{\mathrm{CO_2}} = 0, \quad q_{\mathrm{N_2}} = q^*_{\mathrm{N_2}} \, (C_{\mathrm{N_2}} = 1.0) \end{aligned}$$

TABLE 1: Parameter values in simulation of temperature-dependent Langmuir isotherm

Langmuir parameters	**CO_2**	**N_2**
B_1 (kg/kg)	2.2	0.28
B_2 (1/T)	-0.01	-0.01
B_3 (1/atm)	500	60
B_4 (1/T)	-0.01	-0.02

2. Boundary conditions ($t > 0$):

$$\begin{aligned} &x = 0: \quad U = U_0, \quad V = 0, \quad C_{\mathrm{CO_2}} = 0.1, \\ &C_{\mathrm{N_2}} = 0.9, \quad T_f = T_s = T_w = 330\mathrm{K} \\ &r = 0: \frac{\partial U}{\partial r} = 0, \quad \frac{\partial V}{\partial r} = 0, \quad \frac{\partial C_{\mathrm{CO_2}}}{\partial r} = 0, \\ &\frac{\partial C_{\mathrm{N_2}}}{\partial r} = 0, \quad \frac{\partial T_s}{\partial r} = 0, \quad \frac{\partial T_f}{\partial r} = 0 \\ &r = R: \quad U = 0, \quad V = 0, \quad \frac{\partial C_{\mathrm{CO_2}}}{\partial r} = 0, \\ &\frac{\partial C_{\mathrm{N_2}}}{\partial r} = 0.0, \quad T_f = T_s = T_w = 330\mathrm{K} \end{aligned}$$

3. RESULTS AND DISCUSSIONS

The numerical solution is obtained by employing the finite-volume method. The convective flux term is discretized by the second-order central differencing scheme that is blended with the upwind differencing scheme using the deferred correction method. The SIMPLE algorithm for pressure–velocity coupling is applied. The source term of the equation is linearized in such a way that ensures diagonal dominance in the corresponding discretized equation (Ferziger and Peric, 1999). The discrete equations cannot be solved independently because of the cross-coupling between mass and energy balance equations. Therefore, the iterative method was adopted to solve the temperature and concentration fields. Convergence is checked in terms of the maximum change (10^{-4}) for every variable during the iteration at each time increment. All computations have been carried out for a half-cylindrical reactor with non-uniform grid arrangements. Different grid sizes, such as 50×25 100×50, 200×100, 400×200, and 800×400 have been used in the domain of $L \times R$. As the computational accuracy by taking grid sizes of 200×100, 400×200, and 800×400 are almost the same, we chose the grid size of 200×100 in the computations.

In order to verify the present model, numerical simulation was performed under the same conditions as those of the experiment conducted by Hwang et al. (1995). As shown in Fig. 2, a comparison of outlet CO_2 concentration was made between the numerical solutions and experimental data, in which agreement between the theoretical calculation and experimental measurement can be observed, which validates the present model to some extent.

The four main parameters impacting an adsorption process, such as bulk flow velocity, particle diameter, ef-

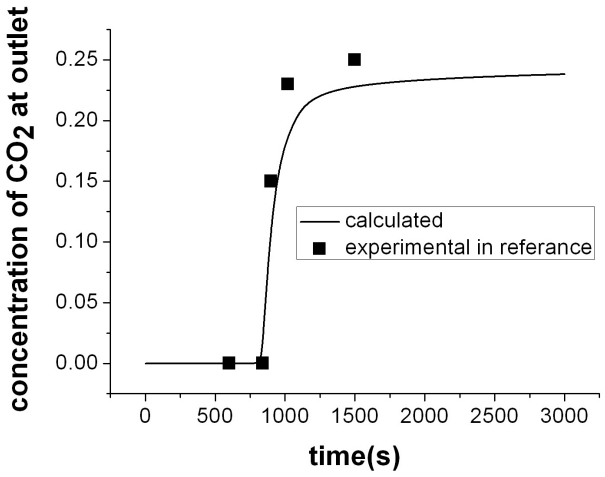

FIG. 2: Comparison between outlet CO_2 concentrations obtained by the present model and the experiment conducted by Hwang et al. (1995)

fective solid thermal conductivity, and specific heat of adsorbent, are analyzed in the following discussions.

3.1 Effect of Bulk Flow Velocity

The influences of the bulk flow velocity on the transport and adsorption characteristics are shown in Figs. 3–6. In Fig. 3 it can be seen that the pressure drop in the packed bed filled with adsorbent increases with the increase of

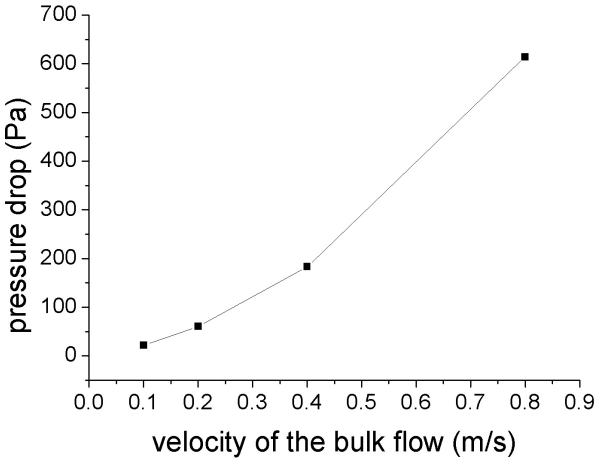

FIG. 3: Effect of bulk flow velocity on the pressure drop between the inlet and outlet

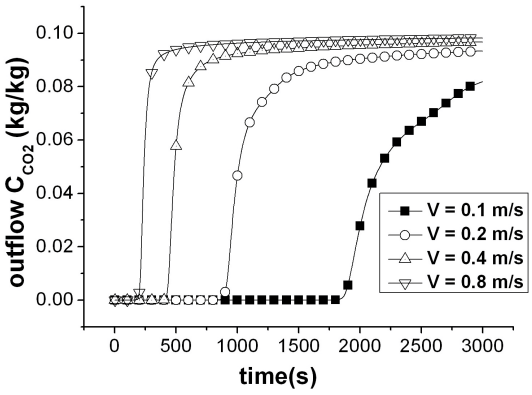

FIG. 4: Effect of bulk flow velocity on CO_2 concentration at the outlet

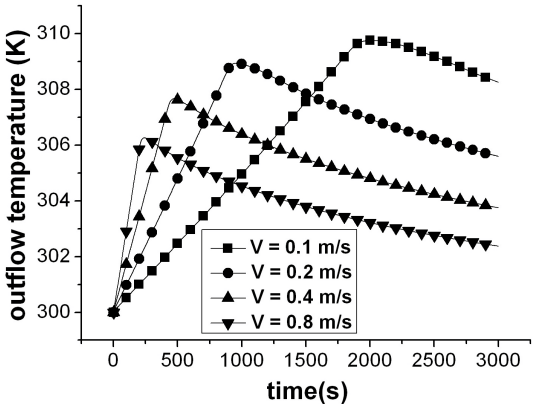

FIG. 5: Effect of bulk flow velocity on outlet fluid temperature

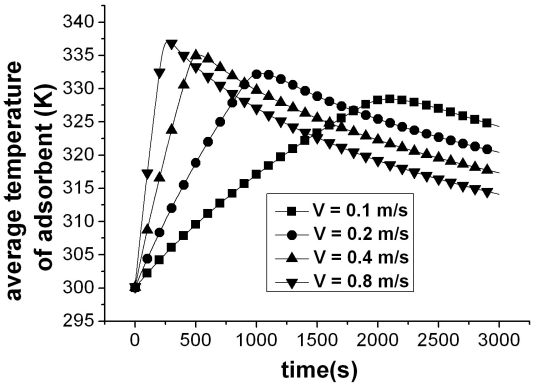

FIG. 6: Effect of bulk flow velocity on average adsorbent temperature

bulk flow velocity, which indicates that more energy is consumed. Figure 4 shows that the larger the bulk flow velocity, the shorter the adsorption time will be. Thus the transition point of the breakthrough curve appears earlier. Therefore, increasing the bulk flow velocity can change the capacity of per-volume adsorbent. Figures 5 and 6 demonstrate that the outlet fluid temperature and average adsorbent temperature increase more rapidly with the increase of bulk flow velocity in the upgoing stage of curves. However, the maximum outlet fluid temperature decreases with an increase of the bulk flow velocity, while this tendency is inversed for the maximum average adsorbent temperature. The reasons for those phenomena can be explained as the increase of the average adsorbent temperature being dependent on the release rate of adsorption heat, the heat transfer rate between solid and fluid and the heat capacity of the solid adsorbent while the increase of bulk fluid temperature depends on the heat transfer rate between solid and fluid and the heat capacity of fluid. If the bulk flow velocity is higher, the adsorption rate will increase, and adsorption-generated heat will release more quickly, which leads to a quicker increase in the solid adsorbent temperature Meanwhile, a higher bulk flow velocity results in a relatively shorter time for fluid residence. Thus heat exchange between fluid and adsorbent is not sufficient, which leads to a lower outlet fluid temperature.

3.2 Effect of Particle Diameter

Figures 7–10 display the effect of the particle diameter of adsorbent on the transport and adsorption characteristics of the packed bed. From Fig. 7 it can be seen that pressure

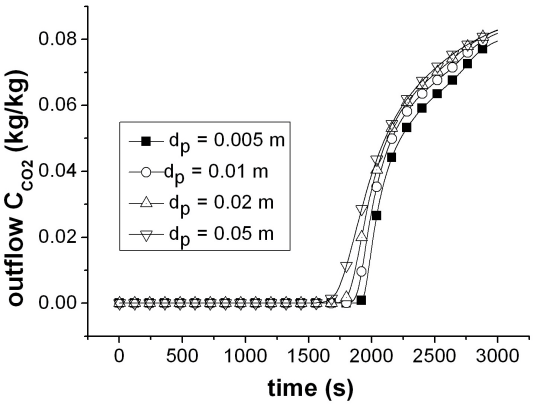

FIG. 8: Effect of particle diameter on outlet CO_2 concentration

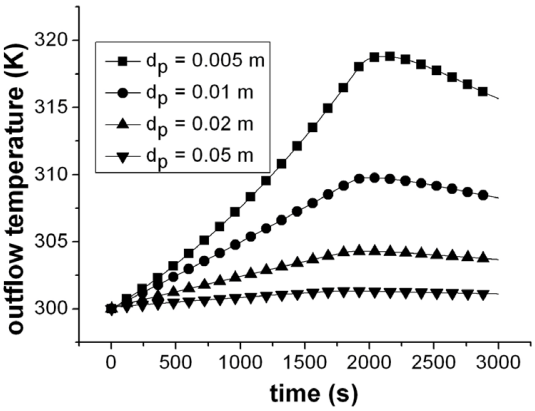

FIG. 9: Effect of particle diameter on outlet fluid temperature

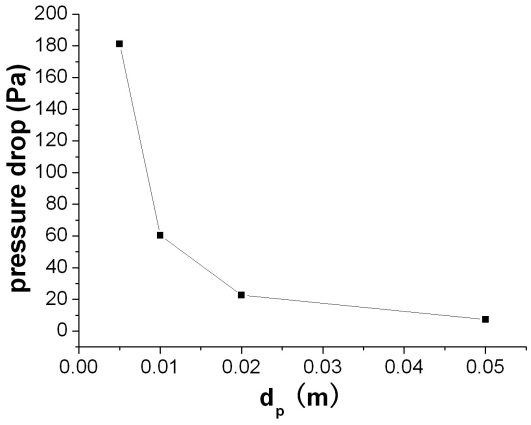

FIG. 7: Effect of particle diameter on the pressure drop between the inlet and outlet

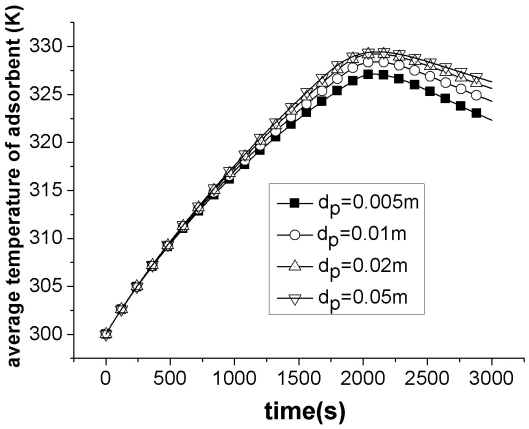

FIG. 10: Effect of particle diameter on average adsorbent temperature

drop decreases greatly with an increase of the particle diameter. It is expected that the permeability of the packed bed increases significantly when the particle diameter becomes larger. This indicates that adopting bigger adsorbent particles can save more energy. Figure 8 shows that the larger the particle diameter, the higher the CO_2 concentration in the outflow will be. It is noted from Fig. 9 that the outlet fluid temperature increases more slowly, as the particle diameter increases, while this tendency is inversed for the average adsorbent temperature shown in Fig. 10. It is expected that when other conditions are fixed, the heat and mass transfer coefficients decrease with the increase of the particle diameter. In the case of larger particles, the increase of average adsorbent temperature leads to a lower equilibrium adsorption quantity. Consequently the adsorption performance will be slightly worse.

3.3 Effect of Effective Solid Thermal Conductivity

As shown in Fig. 11, the time it takes until the appearance of CO_2 in the outflow is almost the same for different curves. After that, however, the outlet CO_2 concentration increases, and its increase rate is relatively slower when $\lambda_{s,\text{eff}}$ is larger. As shown in Figs. 12 and 13, for both the outlet fluid temperature and the average adsorbent temperature the increase rates are also relatively slower when $\lambda_{s,\text{eff}}$ is larger. It can be explained as follows: when effective solid thermal conductivity $\lambda_{s,\text{eff}}$ is raised, more adsorption heat is transferred to the surroundings, which makes the average adsorbent temperature increase more slowly and the equilibrium adsorption quantity increase

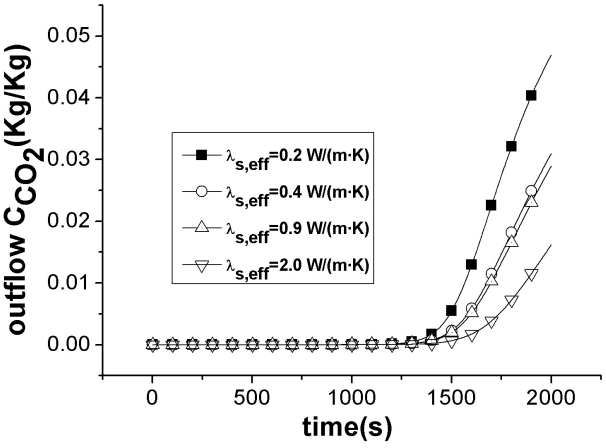

FIG. 11: Effect of $\lambda_{s,\text{eff}}$ on outlet CO_2 concentration

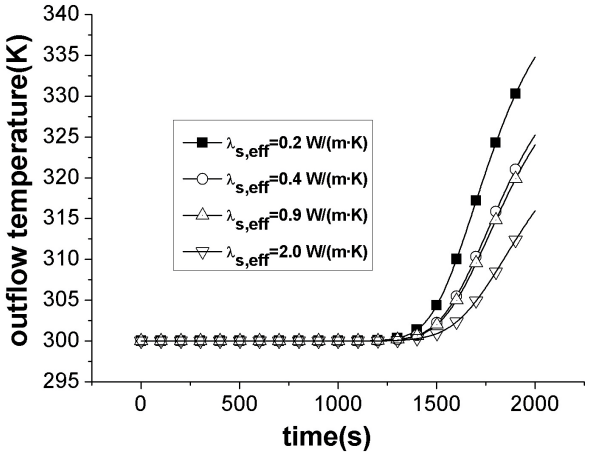

FIG. 12: Effect of $\lambda_{s,\text{eff}}$ on outlet fluid temperature

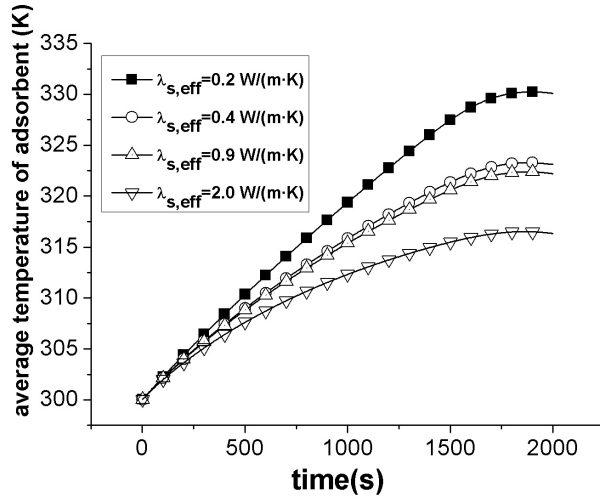

FIG. 13: Effect of $\lambda_{s,\text{eff}}$ on average adsorbent temperature

As a result, the adsorption performance of the packed bed will be improved.

3.4 Effect of Solid Specific Heat

Figures 14–16 demonstrate that when the solid specific heat is larger it takes more time until the appearance of CO_2 in the outflow, and the outlet CO_2 concentration, outlet fluid temperature and average adsorbent temperature increase more slowly. These phenomena can be explained

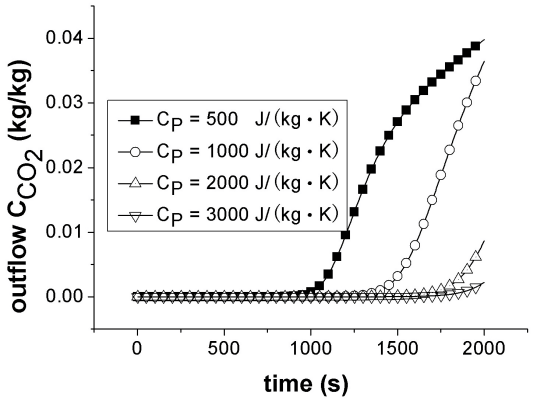

FIG. 14: Effect of solid specific heat on outlet CO_2 concentration

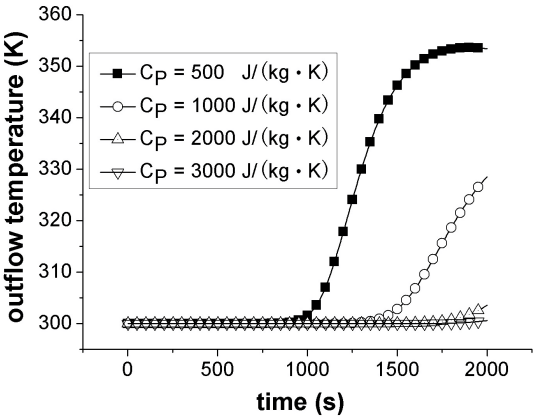

FIG. 15: Effect of solid specific heat on outlet fluid temperature

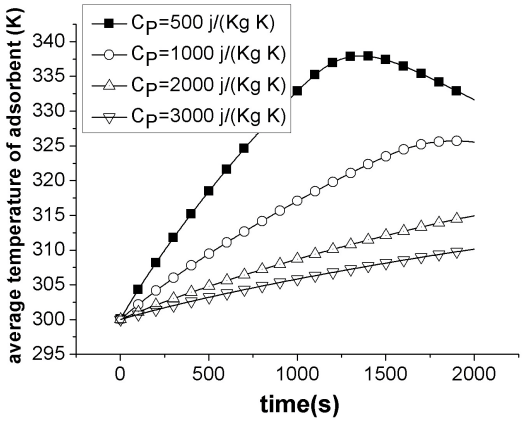

FIG. 16: Effect of solid specific heat on average adsorbent temperature

as follows: when the same amount of heat is absorbed, higher solid specific heat means larger heat capacity of the adsorbent which results in a smaller temperature swing Thus, according to the temperature-dependent Langmuir isotherm, the equilibrium adsorption quantity increases. Therefore, more gas mixtures can be separated and the purity of the production can be raised by increasing the solid specific heat

4. CONCLUSIONS

A local thermal non-equilibrium mathematical model describing the coupled heat and mass transfer in a porous adsorbent bed was established. The model was solved by the finite-volume method and verified through the comparison between simulation results and experimental data reported by other researchers. The effects of the bulk flow velocity, particle diameter, effective solid thermal conductivity and specific heat of the adsorbent were investigated numerically. The computation results show that (1) increasing the bulk flow velocity can enhance the capacity of per-volume adsorbent, but worsen the heat transfer performance and consume more energy; (2) increasing the particle diameter can slightly worsen heat and mass transfer performance, but flow resistance decreases significantly; (3) adsorption performance can be slightly improved when the effective solid thermal conductivity becomes larger; and (4) adsorption performance can be significantly improved when the solid specific heat is increased, while energy consumption remains almost the same. Those results may provide some useful information for operating a PSA process.

ACKNOWLEDGEMENTS

This work was funded by the National Key Basic Research Development Program of China (2007CB206903) and the Natural Science Foundation of China (51036003).

REFERENCES

Amiri, A. and Vafai, K., Transient analysis of incompressible flow through a packed bed *Int. J. Heat Mass Transfer*, vol. **41**, pp. 4259–4279, 1998.

Carta, G., The linear driving force approximation for cyclic mass transfer in spherical pellets, *Chem. Eng. Sci*., vol. **48**, pp. 622–625, 1993.

Cheng, P., Heat transfer in geothermal systems, *Adv. Heat Transfer*, vol. **14**, pp. 1–105, 1978.

Ergun, S., Fluid flow through packed columns, *Chem. Eng. Prog*., vol. **48**, pp. 89–94, 1952.

Ferziger, J. H. and Peric, M., *Computational Methods for Fluid Dynamics*, New York: Springer, 1999.

Glueckauf, E. and Coates, J. I., Theory of chromatography. Part IV: The influence of incomplete equilibrium on the front boundary of chromatograms and on the effectiveness of separation, *J. Chem. Soc.*, vol. **29**, pp. 1315–1321, 1947.

Harlick, P. J. E. and Tezel, F. H., CO_2–N_2 and CO_2–CH_4 binary adsorption isotherms with H-ZSM5: The importance of experimental data regression with the concentration pulse method, *Can. J. Chem. Eng*., vol. **79**, pp. 236–245, 2001.

Hsuen, H. K., An improved linear driving force approximation for intraparticle adsorption, *Chem. Eng. Sci.*, vol. **55**, pp. 3475–3480, 2000.

Hwang, K. S., Jun, J. H., and Lee, W. K., Fixed-bed adsorption for bulk component system Non-equilibrium, non-isothermal and non-adiabatic model, *Chem. Eng. Sci.*, vol. **50**, pp. 813–825, 1995.

Kikkinides, E. S., Yang, R. T., and Cho, S. H., Concentration and recovery of CO_2 from flue gas by pressure swing adsorption, *Ind. Eng. Chem. Res*., vol. **32**, pp. 2714–2720, 1993.

Kim, S. J. and Vafai, K., Analysis of natural convection about a vertical plate embedded in a porous medium, *Int. J. Heat Mass Transfer*, vol. **32**, pp. 665–677, 1989.

Kim, S. J. and Jang, S. P., Effects of the Darcy number, the Prandtl number, and the Reynolds number on local thermal non-equilibrium, *Int. J. Heat Mass Transfer*, vol. **45**, pp. 3885–3896, 2002.

Kim, S. J., Kim, D., and Lee, D. Y., On the local thermal equilibrium in microchannel heats sinks, *Int. J. Heat Mass Transfer*, vol. **43**, pp. 1735–17484, 2000.

Nield, D. A. and Bejan, A., *Convection in Porous Media*, New York: Springer, 1999.

Quintard, M. and Whitaker, S., One- and two-equation models for transient diffusion processes in two-phase systems, *Adv. Heat Transfer*, vol. **23**, pp. 369–464, 1993.

Rees, D. A. S. and Vafai, K., Darcy–Brinkman free convection from a heated horizontal surface, *Numer. Heat Transfer, Part A*, vol. **35**, pp. 191–204, 1999.

Sozen, M. and Kuzay, T. M., Enhanced heat transfer in round tubes with porous inserts *Int. J. Heat Fluid Flow*, vol. **17**, pp. 124–129, 1996.

Steinbery, M., History of CO_2 greenhouse gas mitigation technologies, *Energy Convers Manage*, vol. **133**, pp. 311–315, 1992.

Suzuki, M., *Adsorption Engineering*, New York: Elsevier Science, 1990.

Veldsink, J. W., van Damme, R. M. J., Versteeg, G. F., and van Swaaij, W. P. M., The use of the dusty-gas model for the description of mass transport with chemical reaction in porous media, *Chem. Eng. J*., vol. **57**, pp. 115–125, 1995.

Wakao, N., Kaguei, S., and Funazkri, T., Effect of fluid dispersion coefficients on particle-to-fluid heat transfer coefficients in packed beds, *Chem. Eng. Sci*., vol. **34**, pp. 325–326, 1979.

Whitaker, S., Local thermal equilibrium: An application to packed bed catalytic reactor design, *Chem. Eng. Sci*., vol. **41**, pp. 2029–2039, 1986.